Acoustic Impedance Elements Modeling Oscillating Gas Flow in Micro Channels

T.Veijola

Helsinki University of Technology,
Department of Electrical and Communications Engineering,
P.O.Box 3000, FIN-02015 HUT, Finland, timo.veijola@hut.fi

Abstract

Acoustic impedance models for gas flow in rectangular channels are presented. The models include the effect of slightly rarefied gas (slip-flow region) and the fluid inertia effects. An equivalent circuit is presented that implements the acoustic impedance of a rectangular flow channel. Utilizing these models, acoustic impedance circuits can be constructed to model damping problems, such as the squeezed- film damping of fast oscillating microstructures with dimensions comparable to the mean free path.

Keywords: Gas Flow in Rectangular Channels, Slip flow, Gas Flow in Microstructures, Acoustic Impedance, Oscillating Gas Flow

1 INTRODUCTION

When calculating the flow conductance or the amount of damping in oscillating micromechanical structures, laminar, fully developed Poiseuille flow is usually assumed. In this case, the gas rarefaction can be included in the effective viscosity [1]. This is justified when the flow is steady, or slowly oscillating. However, when the oscillation frequency increases up to a certain frequency, the inertia of the gas will disturb the flow velocity profile, effectively increasing the damping force. This inertia effect has been modeled for a rectangular channel with a large aspect ratio [2], [3], it does not include the contribution of the rare gas that considerably decreases the damping forces in microscale flow channels. Sharipov [4] has included the gas rarefaction effect for the flow in a long rectangular channel with an arbitrary aspect ratio, but only for a steady flow.

In this paper, acoustic impedance models for gas flow in rectangular channels are presented including the effect of slightly rarefied compressible gas (slip-flow region), and the inertia of the gas. A rectangular channel with a large aspect ratio (slot) is first discussed, and then the acoustic impedance for an arbitrary aspect ratio is solved utilizig the compact solution of the Reynolds equation presented in [1]. Finally the resulting equations for the acoustic impedance (admittance) are approximated with equivalent circuits.

1.1 Governing Equations

Assuming a constant pressure drop in a channel with a constant cross-section, Fig. 1, the pressure p and the velocity $v(z)$ are modelled with [3]

$$\rho\frac{\partial v}{\partial t} = -\nabla p + \eta\nabla^2 v \tag{1}$$

where ρ is the density of the gas and η is the viscosity coefficient. Isothermal conditions and laminar flow are assumed and the channel length b is assumed to be smaller than the acoustic wavelength.

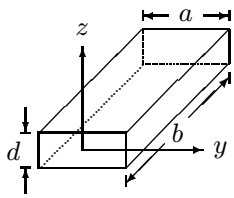

Figure 1: Dimensions of a rectangular flow channel.

2 FLOW IN A NARROW SLOT

First, the flow in a rectangular channel with a large aspect ratio (a/d) is discussed. The frequency-domain solution for the velocity v is of interest for a sinusoidal pressure difference excitation Δp. Since the fluid velocity v, a complex quantity with amplitude and phase, in this case is a function of z only, Eq. (1) becomes

$$\rho\frac{\partial v(z)}{\partial t} = \frac{\Delta p}{b} + \eta\frac{\partial^2 v(z)}{\partial z^2} \tag{2}$$

Due to symmetry about the z-axis, the solution satisfying Eq. (2) is

$$v(z) = C\cosh(qz) + \frac{\Delta p}{j\omega\rho b} \tag{3}$$

where q is the frequency variable $q = \sqrt{j\omega\rho/\eta}$, and C is a constant determined by the boundary conditions.

2.1 Slip Boundary Conditions

Novel results are derived by assuming first-order slip velocity conditions at the boundaries instead of the trivial conditions $v(d/2) = 0$ [5]

$$v(d/2) = -\lambda\frac{\partial v(d/2)}{\partial z}, \tag{4}$$

where λ is the mean free path of the gas molecules. After solving the velocity, the volume flow through a slot of area ad is

$$U = a \int_{-d/2}^{d/2} v(z)\,\mathrm{d}z. \tag{5}$$

The resulting acoustic impedance of a slot of length b is

$$Z_{\mathrm{A1}} = \frac{\Delta p}{U} = \frac{j\omega\rho q b}{a} \frac{1 + q\lambda \tanh(qd/2)}{qd - (2 - q^2 d\lambda)\tanh(qd/2)}. \tag{6}$$

We specify the corner frequency f_{d} as the frequency at which $|qd| = 1$ (the Reynolds number is $\mathrm{Re} = 1$ at frequency f_{d}). This results in

$$f_{\mathrm{d}} = \frac{\eta}{2\pi d^2 \rho}. \tag{7}$$

For an air gap of $1\,\mu$m at atmospheric pressure $f_{\mathrm{d}} = 2.5\,$MHz and for a gap of $10\,\mu$m $f_{\mathrm{d}} = 250\,$kHz.

If $f \ll f_{\mathrm{d}}$, the series expansion of Eq. (6) gives

$$Z_{\mathrm{A0}} \approx \frac{12\eta b}{ad^3(1 + 6K_{\mathrm{n}})} + j\omega \frac{6\rho b}{5ad} \frac{(1 + 10K_{\mathrm{n}} + 30K_{\mathrm{n}}^2)}{(1 + 6K_{\mathrm{n}})^2}, \tag{8}$$

where $K_{\mathrm{n}} = \lambda/d$ is the Knudsen number. If $f \gg f_{\mathrm{d}}$,

$$Z_{\mathrm{A}\infty} \approx \frac{2\eta b}{ad^2\lambda} + j\omega \frac{\rho b}{ad}. \tag{9}$$

For $K_{\mathrm{n}} = 0$, Eq. (8) reduces to result published by Sivian [2] and Wood and Thurston [3],

$$Z_{\mathrm{A0}} \approx R_{\mathrm{A0}} + j\omega L_{\mathrm{A0}} = \frac{12\eta b}{ad^3} + j\omega \frac{6\rho b}{5ad}, \tag{10}$$

but the expansion at frequencies $f \gg f_{\mathrm{d}}$ is different from the expansion in Eq. (9):

$$Z_{\mathrm{A}\infty} \approx \frac{b\sqrt{2\eta\rho\omega}}{ad^2} + j\omega \frac{\rho b}{ad}. \tag{11}$$

2.2 Corrected Model for Large K_{n}

The results given here are based on first-order slip assumptions. However, it is well known that this model is not accurate for large K_{n}. A more accurate model for large K_{n} and for slow velocity has been presented by Fukui and Kaneko [6] and a simple approximation for it is given in [1]. The accuracy of the model given can be improved at frequencies below f_{d}, by multiplying Z_{A1} in Eq. (6) by $(1 + 6K_{\mathrm{n}})/(1 + 9.638K_{\mathrm{n}}^{1.159})$.

2.3 Model Simulations

The influence of the mean free path on the acoustic impedance of a rectangular slot is demonstrated in Fig. 2. An air gap of $1\,\mu$m is assumed. The real part of the impedance is normalized to R_{A0} and the imaginary part is expressed as an inductance normalized to L_{A0}.

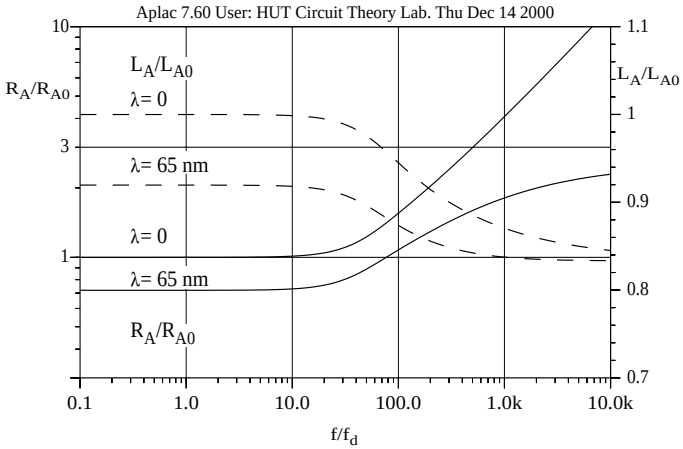

Figure 2: Acoustic resistance (——) relative to R_{A0} and acoustic inductance (– – –) relative to L_{A0} with and without the gas rarefaction effects on a frequency scale relative to f_{d}.

3 FLOW IN A RECTANGULAR CHANNEL

Next, flow in a rectangular channel with an arbitrary aspect ratio is discussed. In this case, Eq. (1) is rewritten with gradient terms for both z- and y-axes:

$$\frac{\eta}{ad}\left[\frac{\partial^2 U(z,y)}{\partial z^2} + \frac{\partial^2 U(z,y)}{\partial y^2}\right] - \frac{\rho}{ad}\frac{\partial U(z,y)}{\partial t} = \frac{\Delta p}{b}. \tag{12}$$

This equation is very similar to the Reynolds equation and in the following, we reuse the existing frequency-domain solution for the Reynolds equation to derive a compact model.

3.1 Continuum Boundary Conditions

When the velocity slip at the surface is ignored, the boundary conditions become trivial and the analytic solution derived for the Reynolds equation can be directly used [1]. This results in an acoustic impedance

$$Z_{\mathrm{A}} = \frac{\Delta p}{U} = \left(\sum_{m,n} \frac{1}{Z_{\mathrm{A},m,n}}\right)^{-1}. \tag{13}$$

where U is the volume velocity through an aperture of $a \times d$, m and n are odd indices, and

$$\begin{aligned} Z_{\mathrm{A},m,n} &= R_{\mathrm{A},m,n} + j\omega L_{\mathrm{A},m,n} \qquad (14) \\ &= \left(\frac{m^2}{d^2} + \frac{n^2}{a^2}\right)\frac{(mn)^2\pi^6\eta b}{64da} + j\omega\frac{(mn)^2\pi^4\rho b}{64da}, \end{aligned}$$

3.2 Slip Boundary Conditions

Equation (12) is now solved applying the slip-flow boundary conditions at the surfaces. Darling et al. [7] have presented an analytic solution for the Reynolds

equation for acoustic conditions at the borders. The boundary condition in Eq. (4) can be written in the form $\nabla U/U = 1/\lambda$, and, are in this case,

$$\frac{k_m d}{2}\tan\frac{k_m d}{2} = \frac{d}{2}\frac{\partial U}{\partial z}\frac{1}{U} = \frac{d}{2\lambda}, \tag{15}$$

$$\frac{k_n a}{2}\tan\frac{k_n a}{2} = \frac{a}{2}\frac{\partial U}{\partial y}\frac{1}{U} = \frac{a}{2\lambda}, \tag{16}$$

where k_m and k_n are the eigenvalues. The eigenvalues cannot be directly solved from Eqs. (15) and (16), thus an analytic approximation is used here, based on the direct iteration. The expressions for $k_m d$ and $k_n a$ are given in Eqs (7) and (8) in [8], where $A_\mathrm{a} = 2\lambda/d$ and $A_\mathrm{b} = 2\lambda/a$, respectively. The acoustic impedance is given again with Eq. (13), where the terms are

$$Z_{\mathrm{A},m,n} = \frac{(k_m d)^2 (k_n a)^2 b}{64 d a B(k_m d) B(k_n a)}\left[(k_m^2 + k_n^2)\eta + j\omega\rho\right], \tag{17}$$

where the function $B(\alpha)$ is

$$B(\alpha) = \left[1 + \frac{\sin\alpha}{\alpha}\right]^{-1}\sin^2\frac{\alpha}{2}. \tag{18}$$

3.3 Simplified Model

A simplified model with only the fundamental term ($m = n = 1$) is considered. It is usable at frequencies below f_d. The simplified expressions for the impedance is

$$Z_\mathrm{A} = Z_{\mathrm{A},1,1} = \left[\frac{\eta_{\mathrm{eff,z}}}{d^2} + \frac{\eta_{\mathrm{eff,y}}}{a^2}\right]\frac{\pi^6 b}{64 d a} + \frac{\pi^4 \rho b}{64 d a}, \tag{19}$$

where

$$\eta_{\mathrm{eff,z}} = \frac{(1 + 6K_\mathrm{a})\eta}{(1 + 6K_\mathrm{d})(1 + 8K_\mathrm{a})}, \tag{20}$$

$$\eta_{\mathrm{eff,y}} = \frac{(1 + 6K_\mathrm{d})\eta}{(1 + 6K_\mathrm{a})(1 + 8K_\mathrm{d})}, \tag{21}$$

where $K_\mathrm{d} = \lambda/d$ and $K_\mathrm{a} = \lambda/a$. A further simplified model for a square channel ($a = d$) with only a single term is

$$Z_\mathrm{A} = Z_{\mathrm{A},1,1} \approx \frac{2\pi^6 \eta b}{64 d^4 (1 + 8K_\mathrm{n})} + j\omega\frac{\pi^4 \rho b}{64 d^2}, \tag{22}$$

where $K_\mathrm{n} = K_\mathrm{d} = K_\mathrm{a}$. This result for resistive losses is in agreement with the slip flow correction for a channel of circular cross-section.

3.4 Corrected Model for Large K_n

The results are given here again based on the first-order slip assumptions. More accurate results for large K_n and for frequencies below f_d have been presented by Sharipov [4] in a tabular form. The accuracy of the model given can be improved at frequencies below f_d by modifying the impedance in Eq. (13) according to the tabulated data in [4].

4 SIMULATION MODEL

Next, the analytic expressions for acoustic impedances are approximately implemented with electrical equivalent circuits. A compact model for squeezed-film damping with end-effects has been presented [8], and here we reuse the same circuit topology.

4.1 Model for Flow in a Narrow Slot

Several attempts to implement the acoustic impedance in Eq. (6) with a simple equivalent circuit for a wide frequency range have failed. Instead, an alternate solution from the Reynolds equation is used here in its 1-dimensional form. When the first-order slip boundary conditions are applied, the terms $Z_{\mathrm{A},m} = R_{\mathrm{A},m} + j\omega L_{\mathrm{A},m}$ in Eq. (13) become

$$Z_{\mathrm{A},m} = \frac{(k_m d)^4 \eta b}{8 d^3 a B(k_m d)} + j\omega\frac{(k_m d)^2 \rho b}{8 d a B(k_m d)}. \tag{23}$$

The acoustic impedance in Eq. (13) is easily implemented as a parallel connection of RL sections. The equivalent circuit topology is shown in Fig. 3.

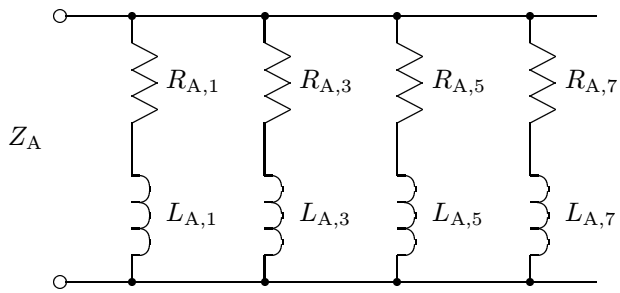

Figure 3: Electrical equivalent circuit approximating the acoustic impedance of a rectangular channel with a high aspect ratio ($d \ll a$) and accounting for the inertial and rarefaction effects.

Figure 4 compares the acoustic resistance and inductance calculated with the electrical equivalent circuit with the analytic expression in Eq. (6)

A simplified model could be implemented by using a single section in the equivalent circuit in Fig. 3 and using the component values given in Eq. (8).

4.2 Model for Flow in a Rectangular Channel

The equivalent circuit in Fig. 3 can be used also to model the rarefied gas flow through a rectangular aperture, but the component values are now given by Eq. (17). A general equivalent-circuit element for the gas flow in rectangular channels is shown, Fig. 5, including rarefaction, compressibility, and inertial effects.

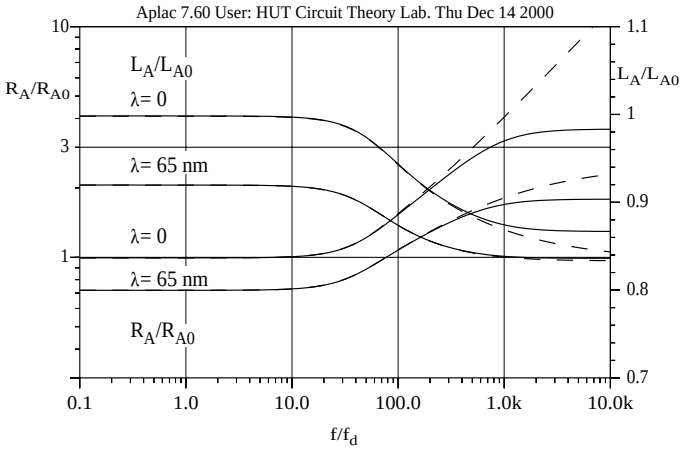

Figure 4: Acoustic resistance and inductance values calculated from the equivalent circuit (——) compared with the analytic expression in Eq. (6) (– – –). Five sections are used in the circuit.

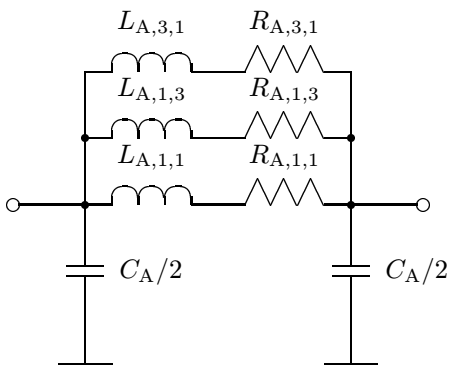

Figure 5: Acoustic impedance element modeling a slice of a rectangular flow channel with an arbitrary aspect ratio including the gas rarefaction, inertial, and compressibility effects. Three RL sections are used here. The acoustic capacitance $C_A = abd/P_A$ is due to the compressible gas.

4.3 Model Applications

The squeezed-film damping problem is well modelled with the Reynolds equation. For small displacements and for rectangular geometry, the Reynolds equation can be analytically solved and implemented as an electrical equivalent circuit [1]. For more complicated geometry, an FD method can be applied.

The Reynolds equation is valid for small Reynolds numbers only. The validity range of the compact squeezed-film damper model in [1] can be extended to include the inertia effects by simply replacing the damping resistors in the model with impedances according to Eq. (23). This approach is justified by the fact that the inertia effects change the velocity distribution of the flow, just like the gas rarefaction effect does.

5 CONCLUSIONS

Acoustic impedance models with inertial effects for slightly rarefied gas flow (slip-flow regime, $K_n < 1$) in rectangular channels with large and arbitrary aspect ratios were given. At frequencies below f_d, the models can be corrected to be valid at arbitrary K_n, but the validity of this model at frequencies well above f_d for large K_n is not known. Simplified models that are usable for frequencies below f_d were also given.

Utilizing these models, acoustic impedance circuits can be constructed to model damping problems, such as the squeezed- film damping of fast oscillating microstructures with dimensions comparable to the mean free path.

The same modelling approach could be utilized to derive acoustic impedance models for channels with a circular cross-section, when the gas rarefaction and inertial effects are to be accounted for.

REFERENCES

[1] T. Veijola, H. Kuisma, J. Lahdenperä, and T. Ryhänen, "Equivalent Circuit Model of the Squeezed Gas Film in a Silicon Accelerometer," *Sensors and Actuators A*, vol. 48, pp. 239–248, 1995.

[2] L. J. Sivian, "Acoustic Impedance of Small Orfices," *Journal of the Acoustical Society of America*, vol. 7, pp. 94–101, 1935.

[3] J. K. Wood and G. B. Thurston, "Acoustic Impedance of Rectangular Tubes," *Journal of the Acoustical Society of America*, vol. 25, pp. 858–860, 1953.

[4] F. Sharipov, "Rarefied Gas Flow Through a Long Rectangular Channel," *J. Vac. Sci. Technol. A*, vol. 17, no. 5, pp. 3062–3066, 1999.

[5] A. Burgdorfer, "The Influence of the Molecular Mean Free Path on the Performance of Hydrodynamic Gas Lubricated Bearings," *Journal of Basic Engineering, Trans. ASME*, vol. 81, pp. 94–99, March 1959.

[6] S. Fukui and R. Kaneko, "Analysis of Ultra-Thin Gas Film Lubrication Based on Linearized Boltzmann Equation: First Report — Derivation of a Generalized Lubrication Equation Including Thermal Creep Flow," *Journal of Tribology, Trans. ASME*, vol. 110, pp. 253–262, April 1988.

[7] R. B. Darling, C. Hivick, and J. Xu, "Compact Analytical Modeling for Squeeze Film Damping with Arbitrary Venting Conditions Using a Green's Function approach," *Sensors and Actuators A*, vol. 70, pp. 32–41, 1998.

[8] T. Veijola, K. Ruokonen, and I. Tittonen, "Compact Squeezed-Film Damping Model Including the Open Border Effects," *Proceedings of MSM 2001*, (Hilton Head), April 2001.